Spectral Analysis of Integrated Pressures on Patches with Unsteady Pressure-Sensitive Paint Measurements

Jie Li[1], Patrick J. Moran[2], Jaffar S. Iqbal[3], Nettie H. Roozeboom[2], Alan E. Landmann[3], Christopher E. Henze[2]

[1]*Aerospace Computing, Inc. Mountain View, CA 94043*
[2] *NASA Ames Research Center, Moffett Field, CA 94035*
[3]*The Boeing Company, Seattle, WA 98124*

This paper describes the spectral analysis of integrated pressures on patches of the scale model of the Space Launch System Block 1 cargo vehicle with the Unsteady Pressure-Sensitive Paint measurements, which were collected in the ascent transient aerodynamics test with the Unitary Plan Wind Tunnel 11-by-11-foot Transonic Wind Tunnel in September 2019 at NASA Ames Research Center. The patches are defined with x station values, indicating the position along length of the vehicle, and azimuth angles of the scale model. For each patch, the polygons are determined from the surface cells of the grid of the model, clipped with the edges of the patch, and each of the polygons is divided into triangles. The integrated pressure of the patch is determined as the ratio of the sum of the forces on the triangles over the sum of the areas of the triangles. For each run of the test, the cross power spectral density and magnitude squared coherence are computed from the time series of the integrated pressures on the patches. The results of pressure integration and spectral analysis are presented, and the data consistency of the test is demonstrated. The work described in this paper is a part of NASA's development of a new state-of-the-art uPSP capability in production wind tunnels. **Funding for this research was provided by the NASA Aeroscience Evaluation and Test Capabilities Project.**

Nomenclature

A	= area (unit: inch^2)
ATAT	= SLS Ascent Transient Aerodynamics Test
C	= matrix of Cross Power Spectral Density (unit: psi^2/Hz) of integrated pressures on patches
CPSD	= Cross Power Spectral Density
F	= force (unit: pound)
FFT	= Fast Fourier Transform
FS	= Forward Skirt
f_s	= sample frequency (unit: Hz)
iFrame	= index of frames
iFreq	= index of frequencies
iParent	- index of parent cells
iPatch, jPatch	= index of patches
iPolygon	= index of polygons
iTriangle	= index of triangles
LOX	= liquid oxygen
LVSA	= Launch Vehicle Stage Adapter

M	= Mach number
NaN	= Not a Number
nFrames	= number of frames
nPatches	= number of patches
p	= pressure (unit: psi)
PSD	= Power Spectral Density
PSP	= Pressure-Sensitive Paint
Q	= dynamic pressure of the freestream (unit: psf)
RMS	= root mean square
SLS	= Space Launch System
UPWT	= NASA Unitary Plan Wind Tunnel
uPSP	= Unsteady Pressure-Sensitive Paint
XYZ	= coordinates in x, y, z axes
α, β	= attitude angles
ΔC_p	= constant component removed pressure coefficient (unit: nondimensional)
γ^2	= magnitude squared coherence (unit: nondimensional) of integrated pressures on patches

Notice to Readers

The predicted performance and certain other features and characteristics of the Space Launch System vehicle are defined by the U.S. Government to be Sensitive But Unclassified (SBU). Therefore, values in plots and figure have been either removed or normalized to arbitrary values.

I. Introduction

The technique of Pressure-Sensitive Paint (PSP) is commonly used in the aerospace industry to measure surface pressures on the model of launch vehicles and airplanes in the wind tunnel test (Refs. [1, 2]). Recent research has demonstrated that Unsteady Pressure-Sensitive Paint (uPSP) can be an essential tool for the assessment of the unsteady, aerodynamic phenomena (Refs. [3, 4, 5]). In a wind tunnel test conducted with the Unitary Plan Wind Tunnel (UPWT) at NASA Ames Research Center, by comparing the buffet loads computed using traditional discrete dynamic pressure transducers with those computed using the uPSP measurements, it was verified that uPSP, with fine spatial resolution, would provide an enhanced method for measuring wind tunnel buffet forcing functions of the launch vehicle (Ref. [6]). NASA is developing a new state-of-the-art uPSP capability in production wind tunnels (Refs. [7-14]). The work described in this paper is a part of the campaign.

This paper describes the spectral analysis of integrated pressures on patches of the scale model of the Space Launch System (SLS) Block 1 cargo vehicle with the uPSP measurements, which were collected in the Ascent Transient Aerodynamics Test (ATAT) with the UPWT 11-by-11-foot Transonic Wind Tunnel in September 2019 at NASA Ames Research Center (Ref. [15]). Fig. 1 shows the model with uPSP in the wind tunnel test. The patches are defined with x station values, indicating the position along length of the SLS vehicle, and azimuth angles of the scale model. For each patch, the polygons are determined from the surface cells of the grid of the model, clipped with the edges of the patch, and each of the polygons is divided into triangles. The integrated pressure of the patch is determined as the ratio of the sum of the forces on the triangles over the sum of the areas of the triangles. For each run of the test, the Cross Power Spectral Density (CPSD) and magnitude squared coherence are computed from the time series of the integrated pressures on the patches. The pressure integration is coded in C++ and the spectral analysis is coded in MATLAB. The results were generated with the execution of the compiled C++ and MATLAB codes in parallel on the NASA Pleiades supercomputer.

This paper is organized as follows. In Section 2, a set of patches is defined on the surface of several components of the SLS vehicle. The algorithms of pressure integration and spectral analysis are discussed in Sections 3 and 4, respectively. In Section 5, the results of pressure integration and spectral analysis are presented, and the data consistency of the SLS ATAT is demonstrated. Finally, the conclusions are presented in Section 6.

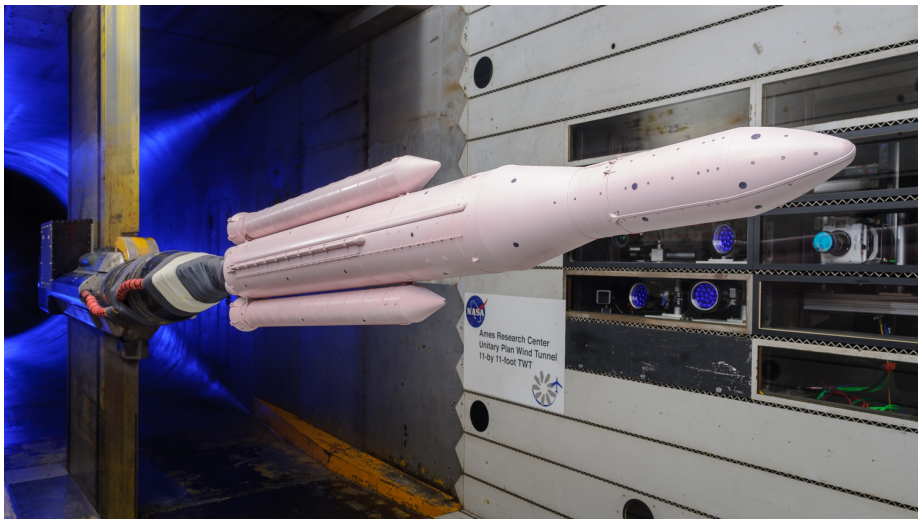

Fig. 1. Scale model of the SLS Block 1 cargo vehicle with the uPSP in the ATAT

II. Definition of a Set of Patches

A set of patches are defined on the surface of the Launch Vehicle Stage Adapter (LVSA), Forward Skirt (FS) and Liquid Oxygen (LOX) tank of the SLS vehicle. Each of the patches is specified by its minimum and maximum x station values as well as its minimum and maximum azimuth angles. Based on the x station values, the patches are grouped into 9 sections, including 4 sections on the LVSA, 2 sections on the FS and 4 sections on the LOX tank. Each section includes 12 patches, and each patch covers 30 degrees of azimuth angle. As a result, a total of 108 patches are defined in the patch set. Fig. 2 shows the set of patches defined on the LVSA, FS and LOX tank of the SLS vehicle. In the figure, the sections of patches on different components of the SLS vehicle are labeled in different colors, and the indices of the 108 patches are illustrated.

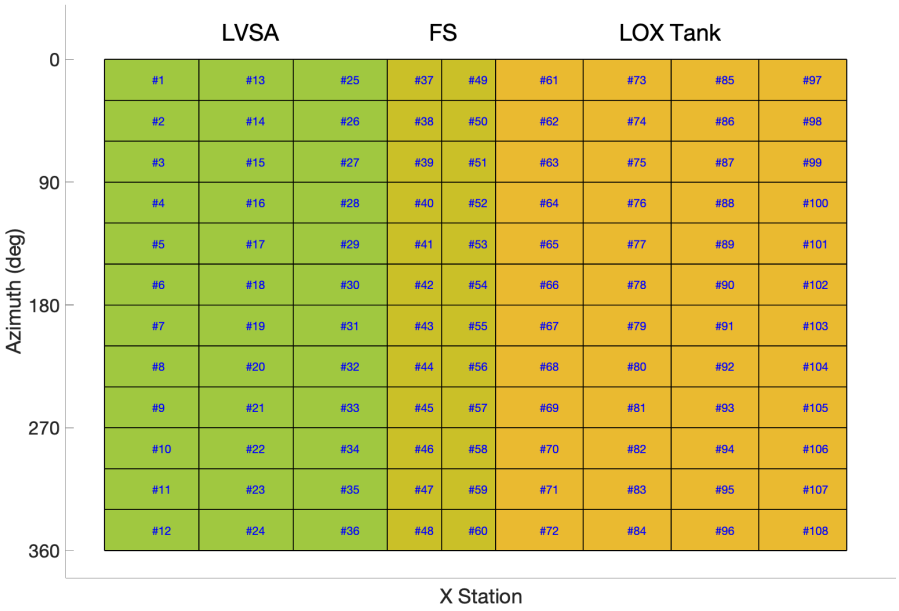

Fig. 2. A set of patches defined on the surface of LVSA, FS and LOX tank of the SLS vehicle.

III. Pressure Integration

The pressure integration was coded in C++. Fig. 3 shows the flowchart of the pressure integration algorithm on one patch.

The inputs of the pressure integration algorithm include the following data files:

- Pressure file, which includes the time series of pressure coefficient ΔC_p (unit: nondimensional) on all vertices of the grid of the model, generated by the uPSP data processing program from the videos taken with 4 Phantom high-speed cameras during the wind tunnel tests. The details of the uPSP data processing program are discussed in Ref. [16]. For each of the vertices, the length of the time series of ΔC_p is equal to the number of frames of the videos, denoted as *nFrame*. Note that several vertices of the grid may be blocked by other components of the SLS vehicle and cannot be seen by any of the 4 cameras, then the ΔC_p values on the vertices are *NaN*s for all frames.

- Wind tunnel file, which includes the wind tunnel test parameters, for example, dynamic pressure Q (unit: psf) of the freestream, etc.

- Grid file, which defines the structured grid of the model.

- Patch file, which includes the minimum and maximum x station values (unit: inch) as well as minimum and maximum azimuth angles (unit: degree) for each of the patches.

From the grid file, a list of surface cells of the grid can be generated, which are called "parent cells". Since the structured grid is used in the SLS ATAT tests, the parent cells are quadrilaterals. The list of parent cells is limited by the specified zones, and the starting and ending zones are given as input parameters of the C++ code.

The edges of a patch are described with 4 planes. The 2 planes perpendicular to the x axis of the model are defined by the minimum and maximum x station values, and the other 2 planes passing the x axis are defined by the minimum and maximum azimuth angles (the x axis of the model is defined as the symmetric axis of the SLS vehicle along the length). Each of the planes divides the 3-dimensional space into 2 parts: positive and negative. The part in the direction of the normal vector of the plane is defined as positive.

Fig. 4 illustrates how the polygons for the integration are determined from the parent cells and the planes of the patch edges. In the figure, the parent cells are illustrated as quadrilaterals in blue and the planes of the patch edges are illustrated as the thick orange lines. The vertices of the grid are labeled as black dots and the new vertices generated when the parent cell is clipped by the plane of the patch edge are labeled as red dots. The areas for the integration are labeled as polygons in green. As shown in Figs. 4(a) and 4(e), when all vertices of a parent cell are in the positive part of a plane, the polygon is the same as the parent cell, which is a quadrilateral; when all vertices of a parent cell are in the negative part of a plane, no polygon is generated for the integration. However, when several vertices of a parent cell are in the positive part of a plane and the other vertices are in the negative part, the polygon for the integration may be triangle, quadrilateral or pentagon, as shown in Figs. 4(b)-4(d), depending on the relative position of the parent cell to the plane.

Fig. 5 shows the vertices of polygons in the set of patches defined in Section 2, where the vertices of the grid are labeled as blue dots, and the new vertices generated in clipping are labeled as red dots. The cyan dots illustrate the vertices on which the pressure coefficients ΔC_p are *NaN*s. In the figure, the regions blocked by the nose of the solid booster rockets can be seen.

The vertices of a polygon are generally not on a plane. As shown in Fig. 6, each of the polygons is divided into triangles, and the force on each of the triangles is computed from the pressure coefficient of the triangle, dynamic pressure and the area of the triangle. The pressure coefficient of a triangle is determined from the pressure coefficients of its corresponding polygon and parent cell. At a specific frame, the pressure coefficient ΔC_p (unit: nondimensional) of a parent cell is defined as the mean of the ΔC_p values on its 4 vertices at the same frame. The pressure coefficients

ΔC_p of a polygon and all triangles divided from the polygon are defined to be equal to ΔC_p of the parent cell of the polygon. If ΔC_p on any of the 4 vertices of a parent cell is *NaN*, all triangles of the polygon generated from the parent cell are labeled as "invalid" and excluded from the pressure integration.

The integrated pressures on a patch are computed for each of the frames separately. The integrated pressure (unit: psi) on Patch #*iPatch* at Frame #*iFrame* is determined as the ratio of the sum of the forces (unit: pound) on the triangles over the sum of the areas (unit: inch^2) of the triangles, as shown below

$$p_{iFrame,\ iPatch} = F_{iFrame,\ iPatch} / A_{iPatch}\ , \tag{1}$$

where

$$F_{iFrame,\ iPatch} = \Sigma_{iTriangle}\ \{\ F_{iFrame,\ iTriangle}\ \} = \Sigma_{iTriangle}\ \{\ \Delta Cp_{iTriangle,\ iFrame} * Q * 1/144 * A_{iTriangle}\ \}\ , \tag{2}$$

$$A_{iPatch} = \Sigma_{iTriangle}\ \{\ A_{iTriangle}\ \}\ . \tag{3}$$

As shown in Eq. (2), a constant 1/144 is introduced to reconcile units of the dynamic pressure Q (in psf) and the area $A_{iTriangle}$ (in inch^2), so the forces on the triangles are in the unit of pound. Note that the summations in Eqs. (2) and (3) are over all "valid" triangles divided from the polygons determined from the parent cells and the 4 planes of the edges of Patch #*iPatch*. For simplicity, the index of the patch, *iPatch*, was removed from the equations in the flowchart of the pressure integration algorithm in Fig. 3.

The output of the pressure integration algorithm is the time series of integrated pressure, at the length of *nFrame*, for each of the patches.

IV. Spectral Analysis

The spectral analysis of integrated pressures on patches was coded in MATLAB. The input of the MATLAB scripts is the time series of integrated pressures on each of the 108 patches, and the outputs include the matrix of CPSD of integrated pressures on patches, magnitude squared coherence between patches, etc. As shown below, the RMS value of the integrated pressure on each of the patches can also be calculated from the matrix of CPSD.

Let *C* denote the 3-dimensional complex matrix of CPSD (unit: psi^2/Hz) of integrated pressures on patches, which was computed with the MATLAB function "cpsd" via Welch's method (Ref. [17]). As illustrated in Fig. 7, the matrix *C* has the size of (*nFFT*/2+1) × *nPatches* × *nPatches*, where *nFFT* is the number of samples to compute the Fast Fourier Transform (FFT) and the CPSD, and *nPatches* = 108.

Let *iPatch* and *jPatch* denote the indices of two patches in the patch set, where *iPatch*, *jPatch* = 1, …, 108. The 1-dimensional complex array *C*(:, *iPatch, jPatch*) gives the CPSD between Patches #*iPatch* and #*jPatch* over the frequency ranging from 0 to $f_s/2$, where f_s is the sample frequency (unit: Hz). When the indices *iPatch* and *jPatch* are equal, the array *C*(:, *iPatch, iPatch*) is real, which gives the Power Spectral Density (PSD) of Patch #*iPatch*. Based on Parseval's theorem (Ref. [17]), the RMS value of the integrated pressure on Patch #*iPatch* can be computed as following

$$p_{RMS,iPatch} = \sqrt{\sum_{iFreq=1}^{nFFT/2+1} C(iFreq, iPatch, iPatch) \cdot (f_s/nFFT)}\ . \tag{4}$$

Let *iFreq* denote an index of frequency, where *iFreq* = 1, …, (*nFFT*/2+1). The corresponding frequency f_{iFreq} is determined as

$$f_{iFreq} = (iFreq - 1) * f_s / nFFT\ . \tag{5}$$

As illustrated in Fig. 8, *C*(*iFreq, :, :*), which gives the CPSD of integrated pressures on patches at the frequency f_{iFreq}, is a 2-dimensional Hermitian matrix. The 2 diagonal elements of the matrix, *C*(*iFreq, iPatch, iPatch*) and *C*(*iFreq, jPatch, jPatch*), corresponding to the PSD of Patches #*iPatch* and #*jPatch* at the frequency f_{iFreq}, are real numbers and labeled as blue squares in the figure, and the 2 off-diagonal elements of the matrix, *C*(*iFreq, iPatch, jPatch*) and *C*(*iFreq, jPatch, iPatch*), corresponding to the CPSD between Patches #*iPatch* and #*jPatch* at the frequency f_{iFreq}, are conjugate complex numbers and labeled as red squares. The magnitude squared coherence between Patches #*iPatch* and #*jPatc*h at the frequency f_{iFreq}, denoted as $\gamma^2(f_{iFreq}, iPatch, jPatch)$, can be determined from the above 4 elements of the Hermitian matrix *C*(*iFreq, :, :*) as following

$$\gamma^2(f_{iFreq}, iPatch, jPatch) = \{ C(iFreq, iPatch, jPatch)\, C(iFreq, jPatch, iPatch) \} / \{ C(iFreq, iPatch, iPatch)\, C(iFreq, jPatch, jPatch) \} . \quad (6)$$

Based on Eq. (6), the following properties of the magnitude squared coherence can be derived

$$\gamma^2(f_{iFreq}, iPatch, jPatch) = \gamma^2(f_{iFreq}, jPatch, iPatch) , \quad (7)$$

and

$$\gamma^2(f_{iFreq}, iPatch, iPatch) = 1 . \quad (8)$$

V. Results of the SLS ATAT

The results of pressure integration and spectral analysis of the SLS ATAT were generated with the execution of the compiled C++ and MATLAB codes in parallel on the NASA Pleiades supercomputer. In this section, the results of pressure integration and spectral analysis are presented and the data consistency of the SLS ATAT is demonstrated.

The data shown in Subsections A and B below are from 4 runs of the SLS ATAT, where the 1st and 2nd runs were taken on the 2nd day of the test, and the 3rd and 4th runs were taken on the 3rd and 4th days respectively. The Mach number, denoted as *M*, of the 4 runs is 0.79, 0.84, 0.91, and 1.10 respectively, and the attitude angles α and β of the 4 runs are all 0s.

The data for the consistency check, as shown in Subsection C, are retrieved from 2 sets of runs sweeping over a range of Mach numbers, taken on the 2nd and 3rd days of the SLS ATAT respectively. The attitude angles α and β of the runs are 0s as well.

A. Integrated pressures

Figs. 9(a)-9(d) show the PSD of uPSP pressures on the vertices of a sample patch (Patch #18) and the integrated pressure on the patch of the 4 runs. In the figures, the PSD, in the unit of psi^2/Hz, of the pressures derived from the uPSP measurements on the vertices of Patch #18 is illustrated as the line in different colors, and the PSD, in the same unit, of the integrated pressure on the patch is illustrated as a thicker blue line. It is observed the uPSP pressures on the vertices of the grid are dominated by the shot noise, and the PSD of the integrated pressure on the patch shows the signal-to-noise ratio increases significantly after the integration over the patch.

It is also observed from Figs. 9(a)-9(d) the PSD values of the uPSP pressures on the vertices of Patch #18 are divided in 2 groups, and the PSD values of one group are smaller than those of the other. It turns out the vertices corresponding to the group of smaller PSD values are located in the field-of-view of 2 cameras. After the fusion of the measurements from 2 cameras, the noise level is reduced, and the PSD value decreases.

Figs. 10(a)-10(d) show the RMS values of integrated pressures on the set of patches of the 4 runs, displayed on the grid of x station values and azimuth angles. As expected, it is observed the RMS values of integrated pressures are close on the patches with the same x station values. It is also observed from Figs. 10(a)-10(c) the RMS values on

Patches #37-60 are larger than those on other patches when the Mach number M is 0.79, 0.84 and 0.91. Investigations show the larger RMS values are due to the Prandtl-Meyer expansion shock waves in the region of FS (Ref. [18]).

B. Spectral analysis outputs

Figs. 11(a)-11(d) show the matrices of magnitude squared coherence between patches of the 4 runs at approximately 5% of the sample frequency, f_s. As shown in Eqs. (7) and (8), the matrix of magnitude squared coherence is symmetric, and the diagonal elements of the matrix are all 1s. These properties can be observed in the figures. It is also observed the values of the magnitude squared coherence are larger for some of the elements of the matrix located at the lines parallel to the diagonal. It turns out to be the effect of the coherence in the directions along and cross the streamlines. The coherence along the streamlines results in the larger coherence values along the lines parallel to the diagonal, and the coherence cross the streamlines makes the lines "thicker".

Figs.12(a)-12(d) show the magnitude squared coherence between one reference patch (Patch #18) and all patches in the patch set of the 4 runs. The data shown in Figs 11 and 12 correspond to the same frequency. In fact, the data shown in Fig. 12 is the 18th row or the 18th column of the matrix of magnitude squared coherence shown in Fig. 11, displayed on the grid of x station values and azimuth angles. From Figs. 12(a)-12(d), the coherence in the directions along and cross the streamlines can be easily observed.

C. Data consistency

The data are compared between the runs with the same test parameters (Mach number, attitude angles, etc.) and taken on different days of the SLS ATAT. Figs. 13(a)-13(d) show the PSD of integrated pressures on Patch #18 of the runs taken on the 2nd and 3rd days of the test. The Mach number M is equal to 0.84, 0.86, 0.89 and 0.91 respectively for the data shown in the figures. It is observed the data of the runs taken on different days of the SLS ATAT are consistent.

VI. Conclusions

This paper describes the spectral analysis of integrated pressures on patches of the scale model of the SLS Block 1 cargo vehicle with the uPSP measurements in the SLS ATAT with the UPWT 11-by-11-foot Transonic Wind Tunnel in September 2019 at NASA Ames Research Center. The definition of the patches is provided, and the algorithms of pressure integration and spectral analysis are discussed. The results of pressure integration and spectral analysis are presented, and the data consistency of the SLS ATAT is demonstrated.

Acknowledgement

Funding for this research was provided by the NASA Aeroscience Evaluation and Test Capabilities Project. The authors would like to thank Jennifer Baerny, Bob Ciotti, David Ellsworth, Ross Flach, Lara Lash, David Murakami, Bron Nelson, Victoria Pollard, Jessica Powell, Timothy Sandstorm, Marc Shaw-Lecerf, Thomas Steva, Paul Stremel, Lucy Tang and Thomas Volden for their expertise in the SLS ATAT and development of the uPSP data processing program. The authors would like to thank James Ross, James Bell, Lawrence Hand and Jayanta Panda for their advices in the research.

References

[1] Bell, J. H., Schairer, E. T., Hand, L. A., and Mehta, R.D., "Surface Pressure Measurements Using Luminescent Coatings", *Annual Review of Fluid Mechanics*, Vol. 33, No. 1, 2001, pp. 155-206.

[2] Liu, T. and Sullivan, J. P., *Pressure and Temperature Sensitive Paints*, Springer-Verlag, 2005.

[3] Gregory, J. W., Asai, K., Kameda, M., Liu, T., and Sullivan, J. P., "A Review of Pressure-Sensitive Paint for High-Speed and Unsteady Aerodynamics", *Proceedings of the Institution of Mechanical Engineers, Part G, Journal of Aerospace Engineering*, Vol. 222, No. 2, 2008, pp. 249-290.

[4] Gregory, J. W., Sakaue, H., Liu, T., and Sullivan, J. P., "Fast Pressure-Sensitive Paint for Flow and Acoustic Diagnostics", *Annual Review of Fluid Mechanics*, Vol. 46, 2014, pp. 303–330.
[5] Sellers, M. E., Nelson, M. A., and Crafton, J.W., "Dynamic Pressure-Sensitive Paint Demonstration in the AEDC Propulsion Wind Tunnel 16T", AIAA Paper 2016-1146, 54th AIAA Aerospace Sciences Meeting, San Diego, CA, January 2016.
[6] Schuster, D. M., Panda, J., Ross, J. C., Roozeboom, N. H., Burnside, N., Ngo, C. L., Kumagai, H., Sellers, M. E., Powell, J. M., Sekula, M. K., and Piatak, D. J., "Investigation of Unsteady Pressure-Sensitive Paint (uPSP) and a Dynamic Loads Balance to Predict Launch Vehicle Buffet Environments", NASA Engineering and Safety Center Report TI-14-00962, 2016.
[7] Roozeboom, N. H., Diosady, L. T., Murman, S. M., Burnside, N. J., Panda, J., and Ross, J. C., "Unsteady PSP Measurements on a Flat Plate Subject to Vortex Shedding from a Rectangular Prism", AIAA Paper 2016-2017, 54th AIAA Aerospace Sciences Meeting, San Diego, CA, January 2016.
[8] Panda, J., "Experimental Verification of Buffet Calculation Procedure Using Unsteady Pressure-Sensitive Paint", *Journal of Aircraft*, Vol.54, No. 5, 2017, pp. 1791-1801.
[9] Sellers, M. E., Nelson, M. A., Roozeboom, N. H., and Burnside, N. J., "Evaluation of Unsteady Pressure Sensitive Paint Measurement Technique for Space Launch Vehicle Buffet Determination", AIAA Paper 2017-1402, 55th AIAA Aerospace Sciences Meeting, Grapevine, TX, January 2017.
[10] Roozeboom, N. H., Ngo, C. L., Powell, J. M., Murakami, D. D., Ross, J. C., Murman, S. M., and Baerny, J. K., "Data Processing Methods for Unsteady Pressure-Sensitive Paint Application", AIAA 2018-1031, 56th AIAA Aerospace Sciences Meeting, Kissimmee, Florida, January 2018.
[11] Panda, J., Roozeboom, N.H., and Ross, J. C., "Wavenumber-Frequency Spectra on a Launch Vehicle Model Measured via Unsteady Pressure-Sensitive Paint", *AIAA Journal*, Vol. 57, No. 5, 2019, pp. 1801-1817.
[12] Roozeboom, N. H., Powell, J. M., Baerny, J. K., Murakami, D. D., Ngo, C. L., Garbeff, T. J., Ross, J. C., and Flach, R. L., "Development of Unsteady Pressure-Sensitive Paint Application on NASA Space Launch System", AIAA Paper 2019-3502, AIAA Aviation Forum, Dallas, TX, June 2019.
[13] Sekula, M. K., Piatak, D. J., Rausch, R. D., Ross, J. C., and Sellers, M. E., "Assessment of Buffet Forcing Function Development Process Using Unsteady Pressure Sensitive Paint", AIAA Paper 2019-3503, AIAA Aviation Forum, Dallas, TX, June 2019.
[14] Steva T. B., Pollard, V. J., Herron, A. J., and Crosby, W. A., "Space Launch System Aeroacoustics Wind Tunnel Test Results", AIAA Paper 2019-2202, AIAA Aviation Forum, Dallas, Texas, June 2019.
[15] Roozeboom, N. H., Murakami, D. D., Li, J., Powell, J. M., Baerny, J. K., Stremel, P. M., Volden, T. R., Flach, R. L., Douthitt, A. N., Steva, T. B., Ross, J. C., and Bell, J. H., "Recent Developments in NASA's Unsteady Pressure-Sensitive Paint Capability", AIAA Paper 2020-0516, AIAA SciTech Forum, Orlando, FL, January 2020.
[16] Powell, J. M., Murman, S. M., Ngo, C. L., Roozeboom, N. H., Murakami, D. D., Baerny, J. K., and Li, J., "Development of Unsteady-PSP Data Processing and Analysis Tools for the NASA Ames Unitary 11ft Wind Tunnel", AIAA Paper 2020-0292, AIAA SciTech Forum, Orlando, FL, January 2020.
[17] Stoica, P. and Moses, R., *Spectral Analysis of Signals*, Prentice Hall, 2005.
[18] Lash, E. L., Roozeboom, N. H., Baerny, J. K., and Garbeff, T. J., "Unsteady Spectral Characterization of Shock Wave/Boundary Layer Interactions on a 4% Scale SLS Model using uPSP and Shadowgraph," AIAA Paper 2020-2725, AIAA Aviation Forum, Virtual Event, June 2020.

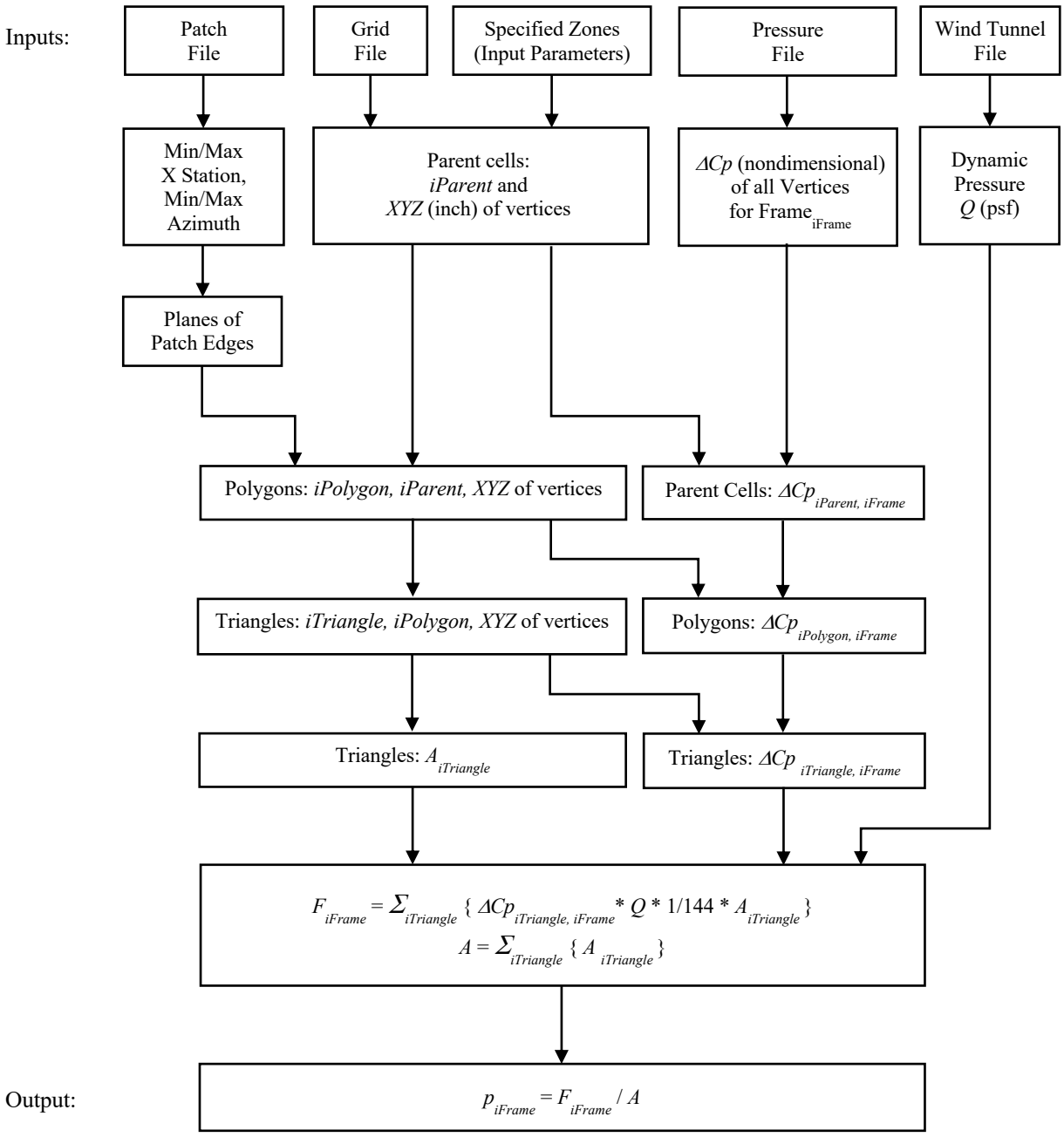

Fig. 3. Flowchart of the pressure integration algorithm on one patch.

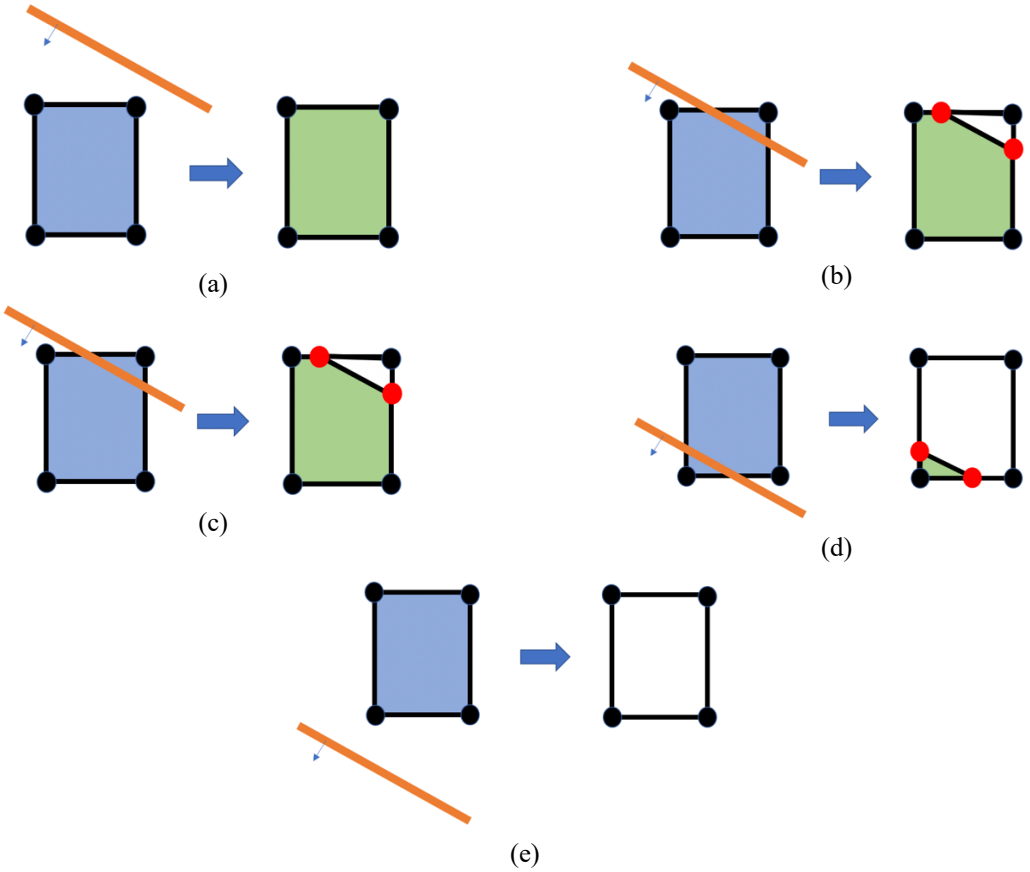

Fig. 4. Polygons for the integration determined with parent cells and the planes of the patch edges. The parent cells are illustrated as quadrilaterals in blue and the planes of the patch edge are illustrated as thick orange lines. The vertices of the grid are labeled as black dots and the new vertices generated in clipping are labeled as red dots. The areas for the integration are labeled as polygons in green.

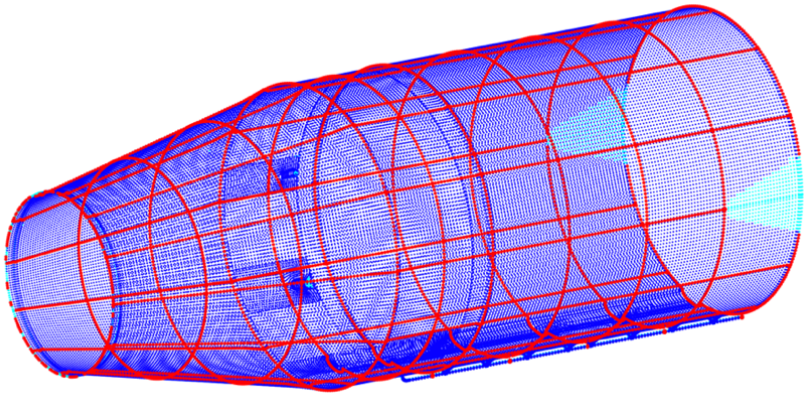

Fig. 5. Vertices of the polygons in the set of patches, where the vertices of the grid are labeled as blue dots and the new vertices generated in clipping are labeled as red dots. The cyan dots correspond to the vertices on which the pressure coefficients are *NaN*s.

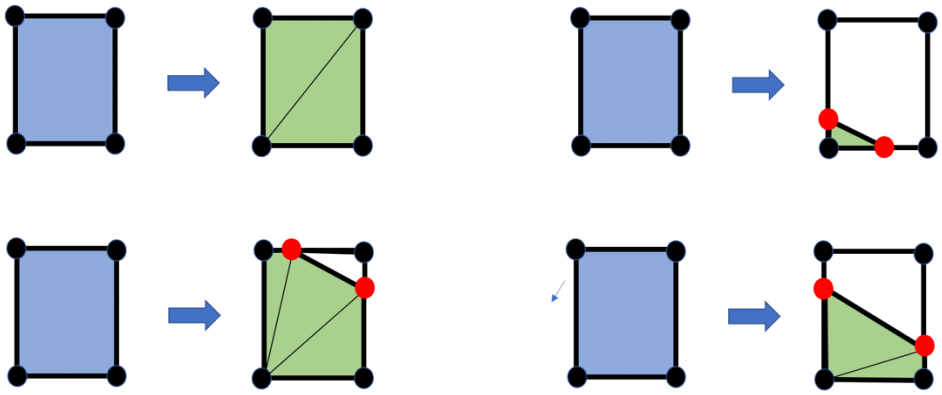

Fig. 6. Each of the polygons is divided into triangles. The force on a triangle is computed from the pressure coefficient of the triangle, dynamic pressure and the area of the triangle.

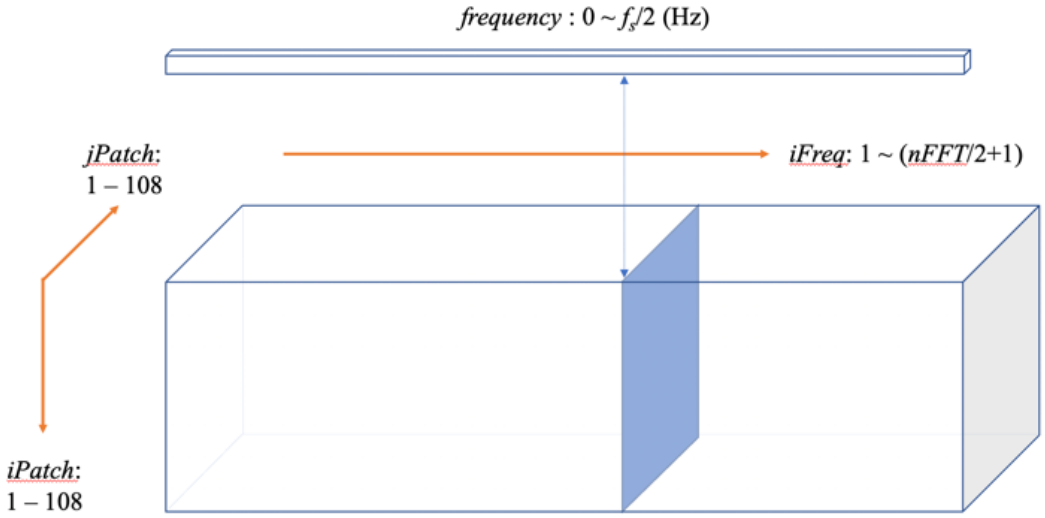

Fig. 7. 3-dimensional matrix of CPSD of integrated pressures on patches.

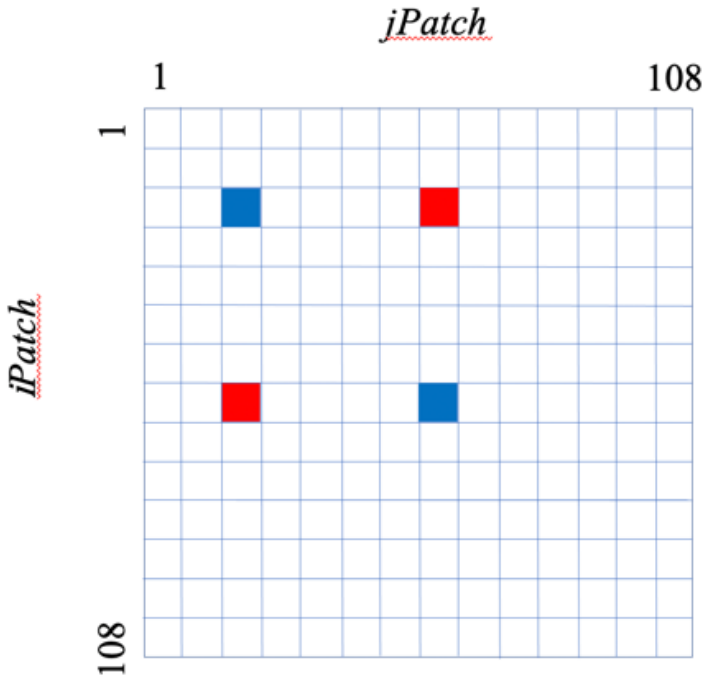

Fig. 8. The CPSD of integrated pressures on patches at a frequency is a 2-dimensional Hermitian matrix, where the 2 diagonal elements, labeled as blue squares, are real numbers and the 2 off-diagonal elements, labeled as red squares, are conjugate complex numbers.

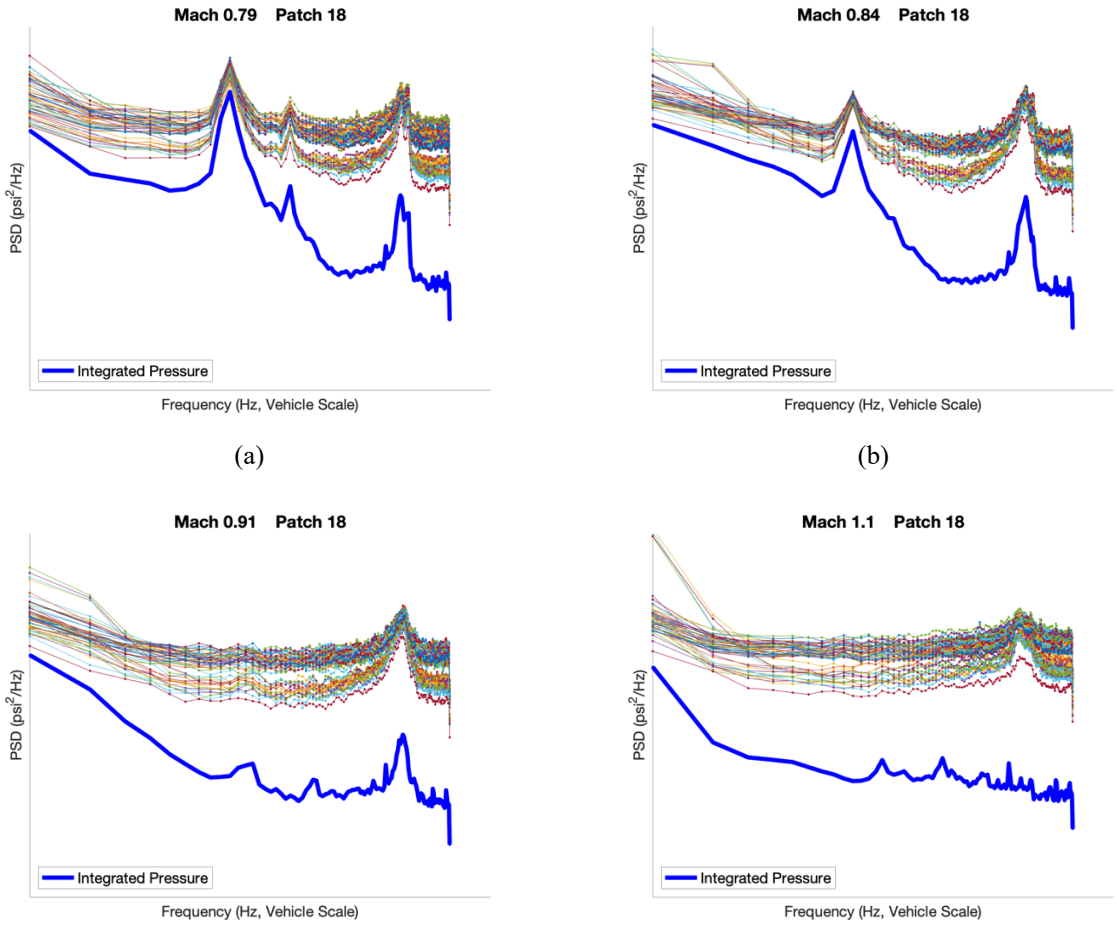

Fig. 9. PSD of integrated pressures on Patch #18 of 4 runs with different Mach numbers. (a) M = 0.79, (b) M = 0.84, (c) M = 0.91, (d) M = 1.10.

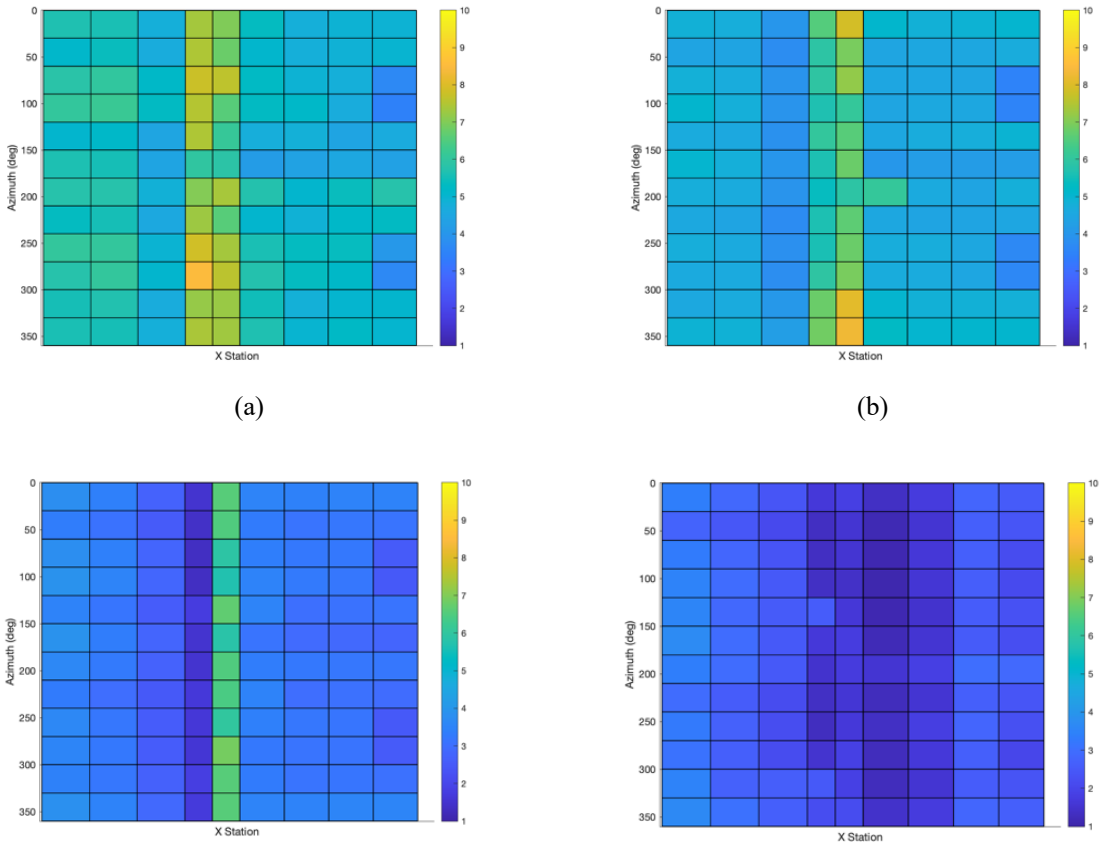

Fig. 10. RMS values of integrated pressures on patches of 4 runs at different Mach numbers. (a) M = 0.79, (b) M = 0.84, (c) M = 0.91, (d) M = 1.10.

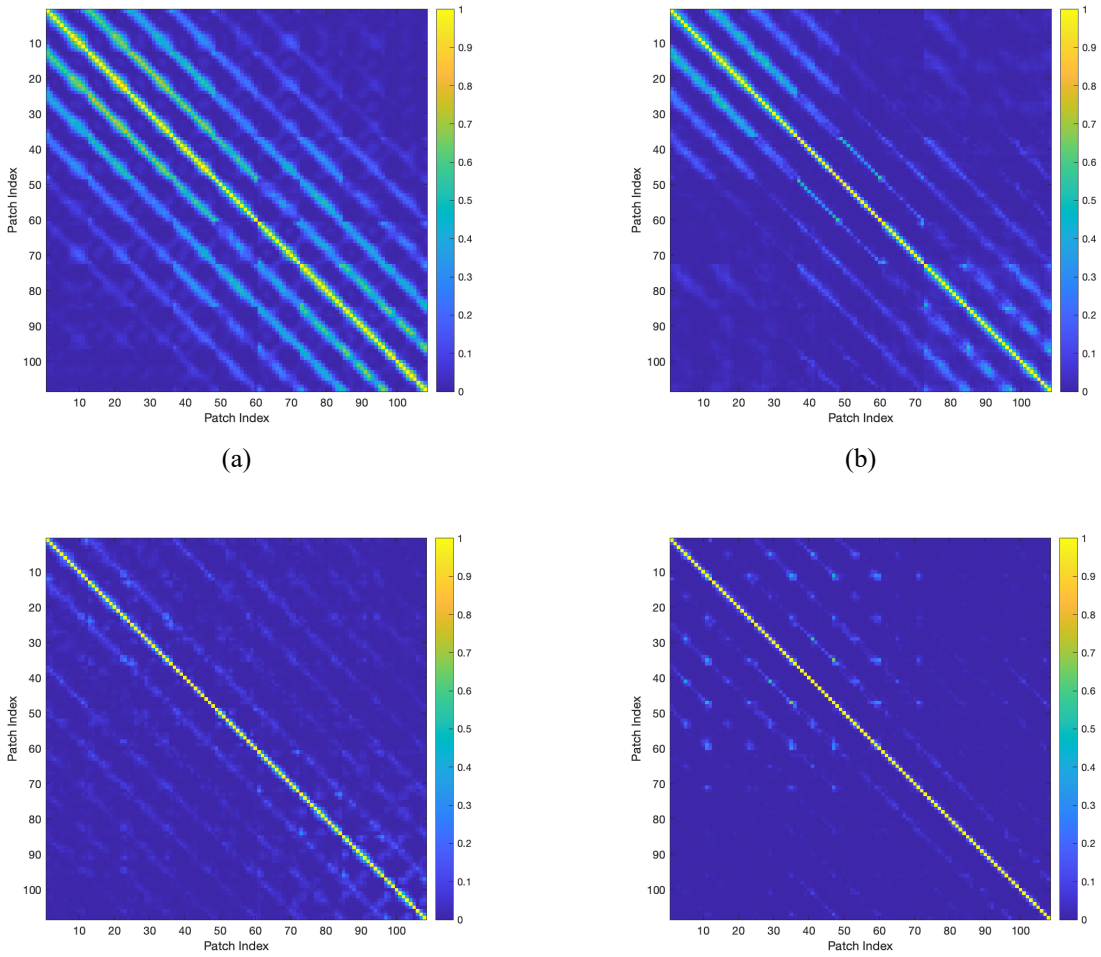

Fig. 11. Matrices of the magnitude squared coherence between patches of 4 runs with different Mach numbers.
(a) M = 0.79, (b) M = 0.84, (c) M = 0.91, (d) M = 1.10.

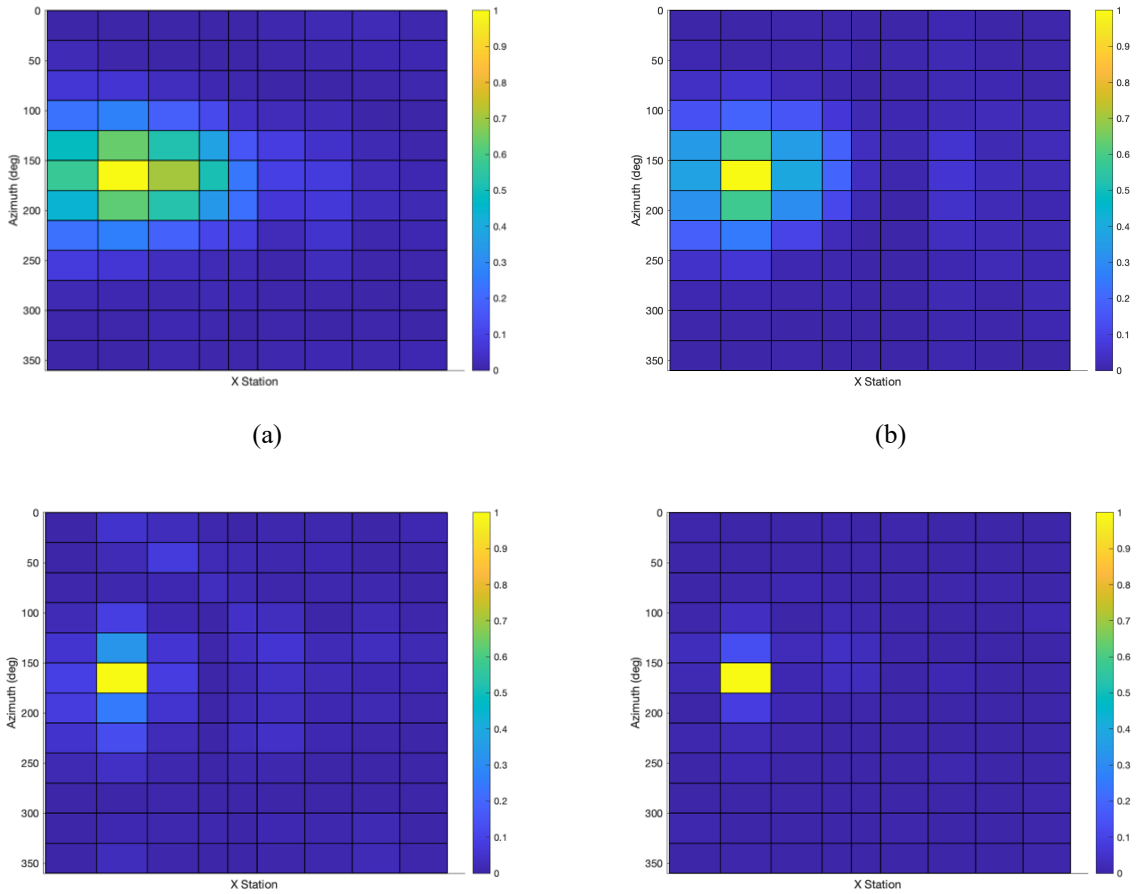

Fig. 12. Magnitude squared coherence between Patch #18 and all patches of 4 runs with different Mach numbers.
(a) M = 0.79, (b) M = 0.84, (c) M = 0.91, (d) M = 1.10.

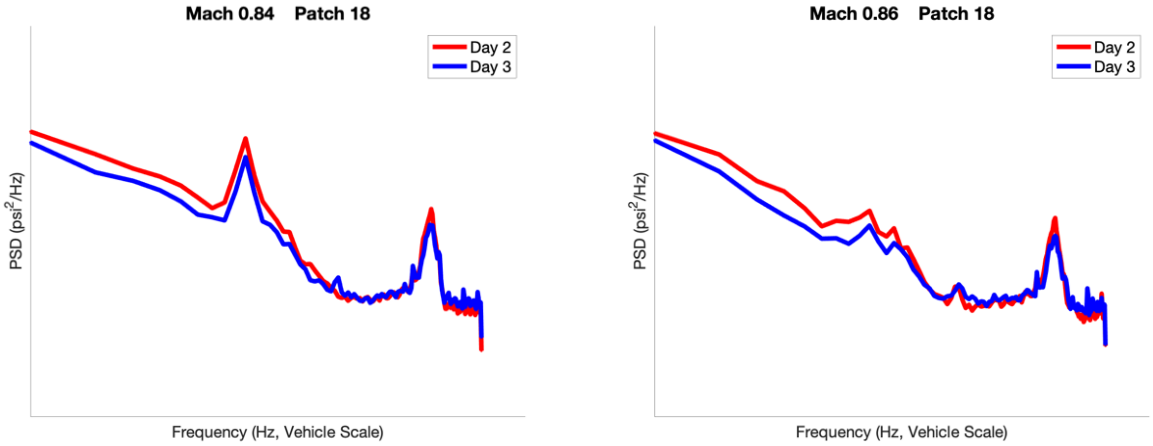

(a) (b)

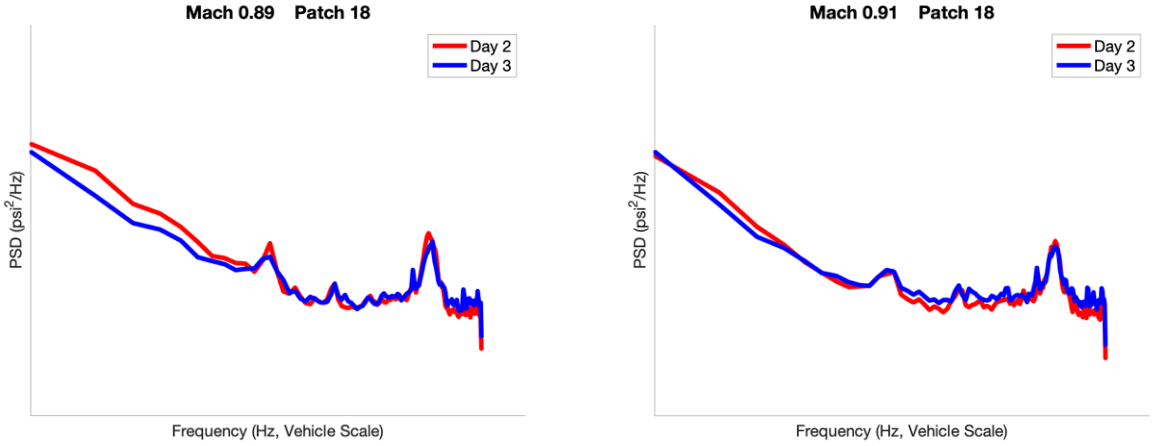

(c) (d)

Fig. 13. PSD of integrated pressures on Patch #18 of the runs with same Mach numbers and taken on the 2nd and 3rd days of the SLS ATAT.
(a) M = 0.84, (b) M = 0.86, (c) M = 0.89, (d) M = 0.91.